Robust control of a sensorless bass-enhanced moving-coil loudspeaker system

Mingsian R. Bai and Hsinping Wu
Department of Mechanical Engineering, National Chiao-Tung University, 1001 Ta-Hseuh Road, Hsin-Chu, Taiwan, Republic of China

(Received 13 November 1998; accepted for publication 5 March 1999)

Moving-coil loudspeakers generally exhibit poor response in the low-frequency range because the diaphragms are unable to produce sufficient volume velocity. To alleviate the problem, this study focuses on enhancing the low-frequency performance of loudspeakers by means of modern control techniques. A self-sensing velocity observer is utilized for producing the cone velocity signal required by the controller. Feedback H_∞ robust control and feedforward H_2 model matching control are employed to simultaneously achieve robust stabilization and tracking performance. The proposed controller is implemented using a combined digital signal processor and operational amplifier circuitry. © *1999 Acoustical Society of America.* [S0001-4966(99)02806-4]

PACS numbers: 43.38.Ja, 43.38.Ar [SLE]

INTRODUCTION

In general, moving-coil loudspeakers exhibit poor response in the low-frequency range because the speaker diaphragms are unable to produce sufficient volume velocity below the mechanical resonance frequency (Borwick, 1994). Insufficient bass content significantly affects the listening quality of audio systems. How to maintain a uniform acoustic output from loudspeakers at very low frequency is a difficult problem. One method of improving the low-frequency response is to increase the radius of the speaker. However, the increase in efficiency is not as great as might be expected, because the mass of the speaker also increases with radius. The low-frequency response can also be enhanced by reducing the stiffness of the suspension, thereby lowering the mechanical resonance frequency. However, if the stiffness of the mechanical system is excessively reduced, its displacement at low frequency becomes very large, which may lead to harmonic distortions resulting from displacement of the voice coil into nonuniform regions of the magnetic field. Although efficiency can also be improved by increasing the magnetic flux density in the air gap (Kinsler *et al.*, 1982), this would result in an undesirable decrease of low-frequency sensitivity. Another conventional approach is electronic compensation, where audio systems are equipped with equalizers to boost the bass output. In doing so, only the magnitude of the low-frequency response is increased, while the phase is distorted even further [unless a linear phase FIR (finite impulse response) digital filter is used]. In contrast to conventional equalizers, this study adopted a different approach of electronic compensation that seeks to increase the bass level without disturbing the phase response so that the waveform distortion is minimized. A very good collection of references on loudspeaker development in last 30 years can be found in Borwick (1994).

The majority of loudspeaker designers to date have focused on the mechanical aspects of loudspeakers (Colloms, 1991). However, an increasing number of researchers are recognizing the potential of using modern control methods to enhance the performance of loudspeakers. Radcliffe and Gogate (1992) employed classical proportional control and velocity feedback to improve low-frequency performance of loudspeakers. Kuriyama and Furukawa (1989) used a feedforward least-mean-square (lms) algorithm to achieve the same purpose. Along the same line, this study attempts to enhance the low-frequency performance by means of modern control techniques, under the electromechanical constraints of the original system. It seeks to optimally increase the magnitude without altering the phase (within a pure delay) of the low-frequency response. To this end, a hybrid structure is employed in the control design. In particular, robust stabilization is achieved using an H_∞ robust feedback controller, whereas tracking performance is maintained via an H_2 model matching feedforward controller. The feedback controller is implemented by using analog operational amplifier (OP) circuitry to avoid excessive delay that might destabilize the closed-loop system. The feedforward controller is implemented on a floating-point digital signal processor (DSP).

The proposed system is different from the other electronically compensated systems (Colloms, 1991) in that this system does not require sensors such as accelerometers or microphones. A self-sensing velocity observer circuit based on the idea of Okada *et al.* (1995) is used for producing the cone velocity signal.

Experimental results show that the proposed system has an enhanced frequency response in the low-frequency region and better tracking performance of time-domain signals than the uncompensated system.

I. MOVING-COIL LOUDSPEAKER

A. Modeling

In this section, a brief review of the model of moving-coil loudspeakers which is also similar to the Thiele-Small's model (Small, 1972) is given. The following definitions are used (Beranek, 1954):

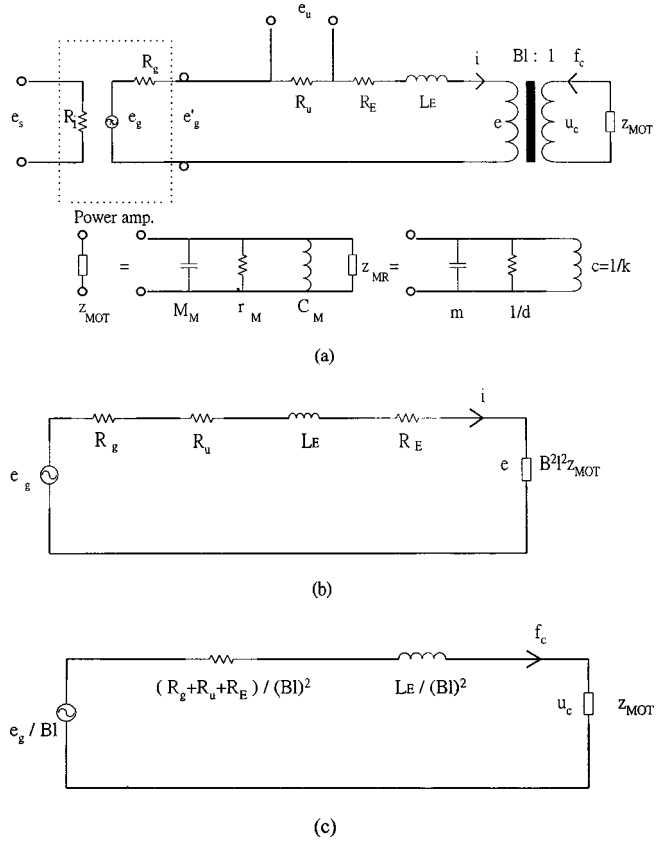

FIG. 1. Electromechanical analogous circuits. (a) Analogous circuit of the mobility type; (b) electrical circuit showing motional electrical impedance; (c) analogous circuit of the mobility type referred to the mechanical side.

e_s, R_i	input voltage and input resistance of the power amplifier
e_g, R_g	open-circuit voltage and internal resistance of the generator
e_g'	output voltage of the power amplifier
R_u	resistance for the velocity observer
e_u	voltage drop across the resistor, R_u
L_E, R_E	inductance and resistance of the coil measured with the voice coil blocked ($u_c = 0$)
Bl	the electromagnetic coupling factor (magnetic flux density×coil length)
e, i	back electromotive force (EMF) and the current of the coil
u_c, f_c	coil velocity and Lorentz force
M_M, C_M, r_M	equivalent mass, compliance, and responsiveness of the mechanical system
Z_{MR}	radiation mobility, $Z_{MR} = (Z_{MR})^{-1}$, Z_{MR} being radiation impedance
Z_{MOT}	motional mobility of mechanical and acoustical systems
m, d, k	effective mass, damping, stiffness of the mechanical and acoustical systems

An equivalent circuit can be drawn by using the mobility analog, as shown in Fig. 1(a). Note that the resistance R_u is inserted in the circuit for measuring current of the coil. The *motional mobility* Z_{MOT} can be expressed in terms of equivalent mass (m), damping (d), and stiffness (k):

$$z_{\mathrm{MOT}} = \frac{1}{j\omega m + d + k/j\omega}. \tag{1}$$

If the circuit of Fig. 1(a) is referred to the electrical side, as shown in Fig. 1(b), the current i can be calculated as

$$i = \frac{e_g}{R_t + j\omega L_E + (Bl)^2 z_{\mathrm{MOT}}}, \tag{2}$$

where the total resistance is defined as $R_t \triangleq R_g + R_u + R_E$. Assume that ($|j\omega L_E| \ll R_t$) is in the low-frequency range and substitute Eq. (1) into (2):

$$\frac{i}{e_g} \cong \frac{(j\omega)^2 m + j\omega d + k}{(j\omega)^2 R_t m + j\omega(R_t d + B^2 l^2) + R_t k}. \tag{3}$$

Equation (3) is a second-order system with a resonance frequency $\sqrt{k/m}$ and damping modified by the factor Bl. Note that a pair of lightly damped zeros are located at the same frequency $\sqrt{k/m}$. Conversely, if the circuit is referred to the mechanical side, as shown Fig. 1(c), the coil velocity u_c can be solved as

$$\begin{aligned} u_c &= \frac{e_g}{Bl}\left[z_{\mathrm{MOT}} \Big/ \left(\frac{R_g + R_u + R_E}{B^2 l^2} + j\omega \frac{L_E}{B^2 l^2} + z_{\mathrm{MOT}} \right) \right] \\ &= e_g Bl \Big/ \left[R_t \left(\frac{1}{z_{M1}} \right) + j\omega L_E \left(\frac{1}{z_{M1}} \right) + B^2 l^2 \right] \\ &= \frac{e_g Bl}{(R_t + j\omega L_E)(j\omega m + d + k/j\omega) + B^2 l^2}. \end{aligned} \tag{4}$$

The low-frequency approximation of coil velocity u_c can be obtained by neglecting the inductance L_E

$$\frac{u_c}{e_g} \cong \frac{j\omega Bl}{(j\omega)^2 R_t m + j\omega(R_t d + B^2 l^2) + R_t k}. \tag{5}$$

Equation (5) represents a second-order system with a dc blocking zero and resonance frequency $\sqrt{k/m}$.

B. Implementation of the velocity observer

In the far field, the sound pressure of a direct-radiator loudspeaker is related to the diaphragm velocity (Beranek, 1954). Hence, cone velocity is selected as the controlled variable in our design. However, direct access of cone velocity requires sensors such as accelerometers that may result in adverse effects of mass loading. A simpler solution is the *self-sensing velocity observer* (Okada *et al.*, 1995). From the electrical side of Fig. 1(a),

$$e_g = (R_t + j\omega L_E) i + Bl u_c. \tag{6}$$

Knowing that $i = e_u / R_u$, we can thus express the coil velocity u_c as

$$u_c = \frac{1}{Bl}\left[e_g - \left(\frac{R_t + j\omega L_E}{R_u} \right) e_u \right]. \tag{7}$$

Hence, a velocity observer can be constructed based on the idea of Eq. (7), provided parameters R_u, R_t, L_E, and Bl have been measured. However, common calibration procedures (Beranek, 1954) that treat these parameters as ideal constants appeared insufficient for our purpose. We use a different approach to accommodate the frequency variation of the parameters. Rewrite Eq. (7) in terms of the output voltage of the power amplifier (e_g')

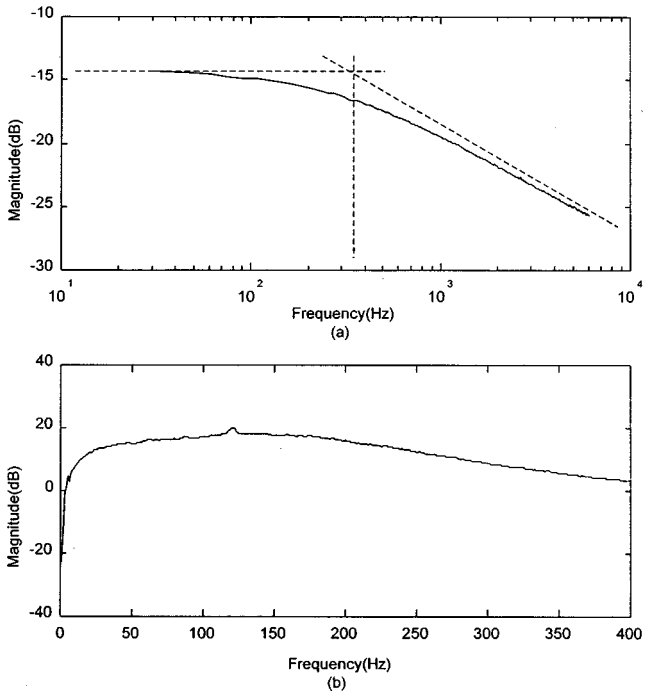

FIG. 2. Frequency responses of electrical parameters. (a) Bode plot of $H(j\omega)=R_u/(R_t'+j\omega L_E)$; (b) $1/Bl$.

$$u_c=\frac{1}{Bl}\left[e_g'-\left(\frac{R_t'+j\omega L_E}{R_u}\right)e_u\right], \tag{8}$$

where $R_t' \triangleq R_u+R_E$. Now, setting $u_c=0$ in Eq. (8) leads to

$$\frac{e_u}{e_g'}=\frac{R_u}{R_t'+j\omega L_E}=\frac{(R_u/R_t')}{1+j\omega/(R_t'/L_E)}\triangleq H(j\omega), \tag{9}$$

where $H(j\omega)$ is the *blocked* frequency response (with the speaker diaphragm held still, i.e., $u_c=0$) between the voltage drop across the current sensing resistor and the output voltage of the power amplifier. The function $H(j\omega)$ is a first-order low-pass function with the corner frequency $\omega_c=R_t'/L_E$ and dc level $H_0=R_u/R_t'$. To satisfy the blocking condition, we simply place a hard rubber stopper firmly against the cone. With R_u pre-specified, R_t' and L_E can be identified from the Bode plot of $H(j\omega)$, i.e.,

$$R_t'=R_u/H_0 \quad \text{and} \quad L_E=R_t'/\omega_c. \tag{10}$$

The Bode plot of $H(j\omega)$ obtained for our system is shown in Fig. 2(a). The remaining work is to identify the factor $(1/Bl)$. Dividing both sides of Eq. (8) by e_s gives

$$\frac{u_c}{e_s}=\frac{1}{Bl}\left[\frac{e_g'}{e_s}-\left(\frac{R_t'+j\omega L_E}{R_u}\right)\frac{e_u}{e_s}\right]. \tag{11}$$

We then measure the coil velocity u_c using a Polytec OFV 2500 laser velocity sensor. Form the frequency responses u_c/e_s, e_g'/e_s, e_u/e_s, and the identified value of $(R_t'+j\omega L)/R_u$, the factor $(1/Bl)$ is determined, as shown in Fig. 2(b). This factor appears to be frequency dependent. This frequency dependence entails the need to treat the factor $(1/Bl)$ in Eq. (8) as a filter so that the magnitude and phase of coil velocity can be accurately described. The resulting velocity observer in Eq. (11) is implemented by an OP circuit (Schaumann *et al.*, 1989), as shown in Fig. 3.

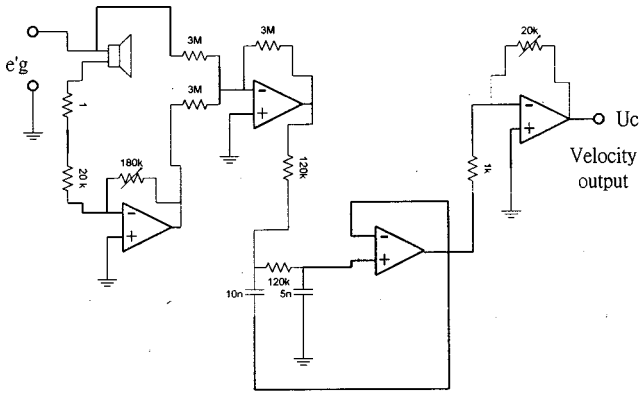

FIG. 3. OP circuit of the self-sensing velocity observer.

II. ROBUST CONTROL DESIGN

The hybrid structure (Aström, 1990) composed of a feedforward controller and a feedback controller is adopted in the control design. The design strategy is first to find an H_∞ feedback controller that stabilizes the open-loop plant, where ''plant'' means ''the controlled system.'' The reason for using a feedback module is to increase robustness against plant uncertainties and perturbations so that the cone velocity is nearly constant (Morari and Zafirou, 1989). Next, a feedforward controller is introduced to achieve tracking performance without degrading the stability of the feedback-compensated system. It is noted that an optimally matched feedforward control is a step beyond merely using a linear phase FIR digital filter that does not take into account the phase response of the plant.

A. H_∞ robust feedback controller

The feedback structure of Fig. 4 is considered. To find an H_∞ controller, we weight the sensitivity function $\tilde{S}(z)$ by $W_1(z)$, the control input $u(k)$ by $W_2(z)$, and the complementary sensitivity function $\tilde{T}(z)$ with $W_3(z)$, where

$$\tilde{S}(z)=\frac{1}{1+P(z)C(z)} \tag{12}$$

and

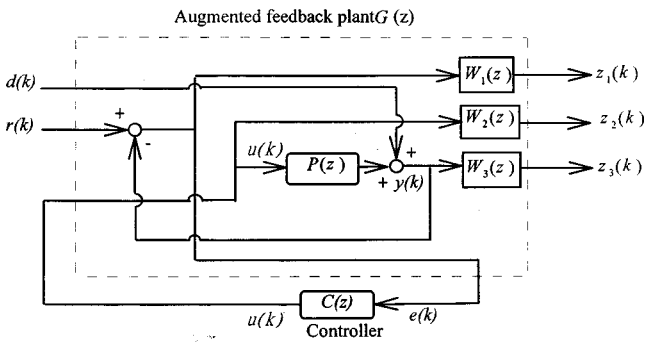

FIG. 4. System diagram of feedback control.

$$\tilde{T}(z)=\frac{P(z)C(z)}{1+P(z)C(z)}. \tag{13}$$

For good disturbance rejection and tracking performance, the nominal performance condition must be satisfied (Doyle *et al.*, 1992)

$$\|\tilde{S}(z)W_1(z)\|_\infty<1. \tag{14}$$

On the other hand, for system stability against plant perturbations, the robustness condition must be satisfied

$$\|\tilde{T}(z)W_3(z)\|_\infty<1. \tag{15}$$

The tradeoff between $\tilde{S}(z)$ and $\tilde{T}(z)$ dictates the performance and stability robustness of the feedback design:

$$\||\tilde{S}(z)W_1(z)|+|\tilde{T}(z)W_3(z)|\|_\infty<1 \tag{16}$$

The input–output relation of the augmented plant of the feedback structure is

$$\begin{bmatrix} Z_1(z) \\ Z_2(z) \\ Z_3(z) \\ E(z) \end{bmatrix}=\begin{bmatrix} W_1(z) & -W_1(z)P(z) \\ 0 & W_2(z) \\ 0 & W_3(z)P(z) \\ 1 & -P(z) \end{bmatrix}\begin{bmatrix} D(z) \\ U(z) \end{bmatrix}, \tag{17}$$

where $Z_1(z)$, $Z_2(z)$, and $Z_3(z)$ are controlled variables, and $P(z)$ is the open-loop plant. The extraneous input $D(z)$ consists of the reference $r(k)$ and disturbance $d(k)$. The signals $U(z)$ and $E(z)$ are the control input to the plant and the measured output from the plant, respectively. In H_∞ theory, the suboptimal condition of the feedback controller reads (Doyle *et al.*, 1992).

$$\left\|\begin{bmatrix} W_1(z)\tilde{S}(z) \\ W_2(z)\tilde{R}(z) \\ W_3(z)\tilde{T}(z) \end{bmatrix}\right\|_\infty<1, \tag{18}$$

where

$$\tilde{R}(z)=\frac{C(z)}{1+P(z)C(z)}. \tag{19}$$

In H_∞ control synthesis, the optimal tradeoff between performance and stability robustness is achieved by tuning the weighting functions $W_1(z)$, $W_2(z)$, and $W_3(z)$. In general, $W_1(z)$ and $W_3(z)$ are chosen as a low-pass function and a high-pass function, respectively. The details of how to select the weighting functions can be found in Bai and Lin (1997).

B. H_2 feedforward model matching controller

Having stabilized the plant $G(z)$ by the feedback controller, the design effort can then be focused on finding a feedforward controller $C(z)$ which makes the plant output track the desired output of a reference model $M(z)$. In our study, $M(z)$ is chosen as the following function:

$$M(z)=\frac{z^{-10}(1.4695-0.0609z^{-1})}{1-0.5305z^{-1}}. \tag{20}$$

Note that the above function contains a pure delay term z^{-10} and a first-order low-pass function. The low-pass function is to attenuate the excessive gain outside the control bandwidth. The pure delay, which will not introduce waveform distortion, is essential in calculating the controller using the model matching principle, and is detailed as follows.

The matching procedure is based on the H_2 criterion. Let the squared error be

$$\epsilon_2^2=\|M(z)-C(z)G(z)\|_2^2, \tag{21}$$

where the 2-norm of a transfer function is defined as

$$\|G(z)\|_2\triangleq\left(\frac{1}{2\pi}\int_{-\pi}^{\pi}|G(e^{j\theta})|^2d\theta\right)^{1/2}. \tag{22}$$

The feedforward model matching problem reduces to finding a stable transfer function $C(z)$ to minimize ϵ_2^2. We perform an *inner–outer factorization* (Doyle *et al.*, 1992) on $G(z)$:

$$G(z)=V_a(z)V_m(z), \tag{23}$$

with $V_a(z)$ being an all-pass function and $V_m(z)$ being a minimum phase function. Substitute Eq. (23) into Eq. (21) and omitting (z) for simplicity, we have

$$\begin{aligned}\epsilon_2^2&=\|M-V_aV_mC\|_2^2=\|V_aV_a^{-1}M-V_aV_mC\|_2^2\\&=\|V_a(V_a^{-1}M-V_mC)\|_2^2=\|V_a^{-1}M-V_mC\|_2^2.\end{aligned} \tag{24}$$

In the last step, the fact that V_a has a bounded constant magnitude on the unit circle is used. Now, decompose $V_a^{-1}M$ as follows:

$$V_a^{-1}M=(V_a^{-1}M)_+ +(V_a^{-1}M)_- , \tag{25}$$

where $(V_a^{-1}M)_+$, and $(V_a^{-1}M)_-$ correspond to the unstable part and the stable part, respectively. Then Eq. (24) can be rewritten into

$$\begin{aligned}\epsilon_2^2&=\|(V_a^{-1}M)_+ +(V_a^{-1}M)_- -V_mC\|_2^2\\&=\|(V_a^{-1}M)_+\|_2^2+\|(V_a^{-1}M)_- -V_mC\|_2^2.\end{aligned} \tag{26}$$

The Pythagoras theorem in Hilbert space is used in the last equality. Thus the optimal $C_{\text{opt}}(z)$ becomes

$$C_{\text{opt}}(z)=V_m^{-1}(V_a^{-1}M)_- . \tag{27}$$

III. EXPERIMENTAL INVESTIGATIONS

The experimental setup is composed of a one-way closed-box woofer with an 8-in. moving-coil direct radiator speaker driven by a 30-W power amplifier, a mid-range speaker, and a tweeter driven by a 25-W power amplifier.

Prior to controller design, the model of the plant $G(z)$ needs to be determined. One way of constructing the plant model is to identify all parameters in Eq. (5). Alternatively, one may use a system identification procedure to construct the model, based on the input data e_g and output data u_c. This paper chose the latter approach which may capture more dynamics overlooked by the low-frequency analytical model in Eq. (5). The comparison in Fig. 5 shows good agreement between the measured frequency response and the regenerated frequency response of the identified plant.

On the basis of the identified plant, the aforementioned H_∞ procedure and H_2 procedure are applied to obtain the optimal feedback controller and feedforward controller, re-

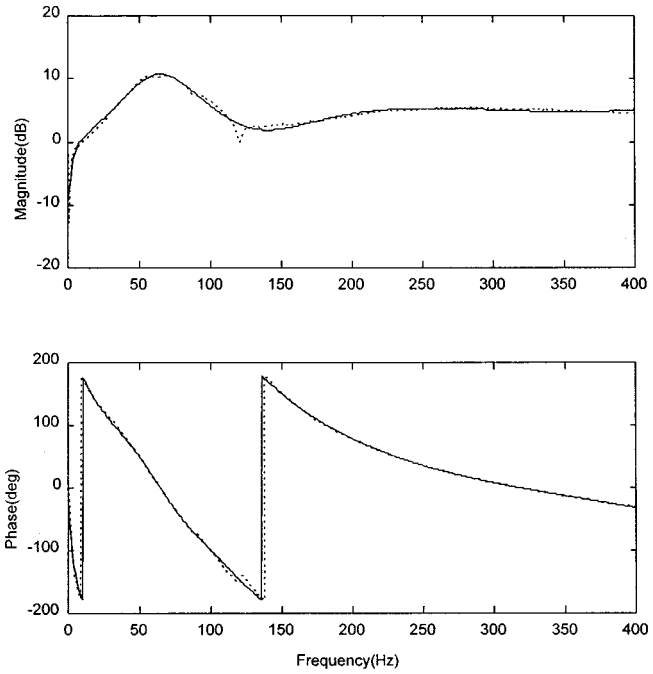

FIG. 5. Comparison between the measured and the regenerated frequency responses of the open-loop plant. Measured data ———; regenerated data —.

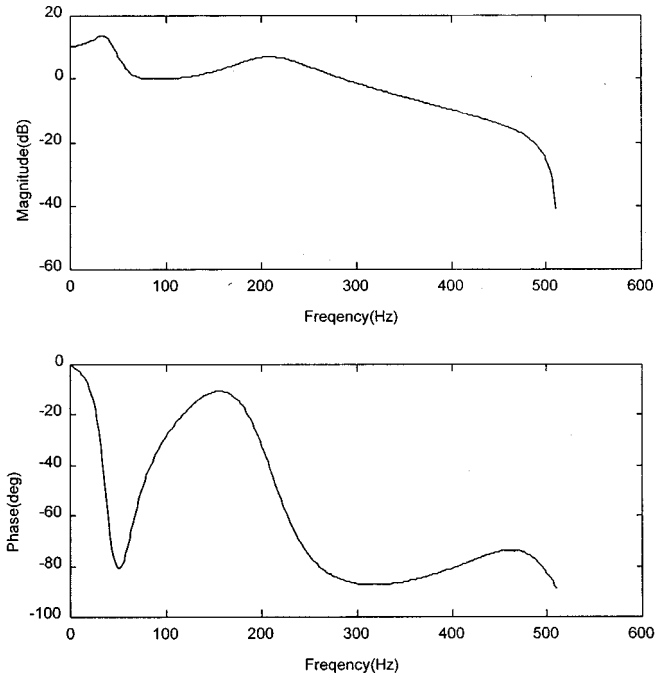

FIG. 7. Frequency response of the H_∞ feedback controller.

spectively. The feedback controller is implemented by an OP circuit to avoid excessive delay, whereas the feedforward controller is implemented by a digital filter on a 32-bit floating-point DSP (TMS320C31) with a sampling rate 2 kHz that is nearly five times of the control bandwidth, which meets the Nyquist sampling criterion. A two-channel 16-bit input/output daughter module is used. The board is equipped with anti-aliasing filters and smoothing filters. The dynamic range of quantization is 90 dB. The total system diagram is shown in Fig. 6. The frequency response of the feedback controller and the associated electric circuit of the analog controller are shown in Figs. 7 and 8, respectively. Prior to the feedforward controller design, the model of the feedback-compensated plant is determined via a frequency-domain identification procedure (Juang, 1994). The measured frequency response and the regenerated frequency response of the compensated plant are compared in Fig. 9. By H_2 optimization, the optimal feedforward controller is found (Fig. 10). As expected, the controller exhibits high gain in the low-frequency range.

The feedback controller and the feedforward controller are hence combined to enhance the bass quality of the audio system. Although coil velocity is the controlled variable in our design, a monitoring microphone is also set in the far field (20 cm away) to evaluate the acoustical performance. The frequency responses for the uncompensated system and the system compensated by the hybrid control are compared in term of the coil velocity and the far-field sound pressure (Figs. 11 and 12). The experimental result shows significant improvement of bass quality by driving the low-frequency limit of the loudspeaker from approximately 60 Hz down to 20 Hz. The magnitude enhancement ranges from 3 dB to 20 dB throughout the 400-Hz control bandwidth. In addition, the phase linearity is not degraded (with a pure delay) because of the electronic compensation. Note that there is a hump around 10 dB. This peculiar result is done on purpose

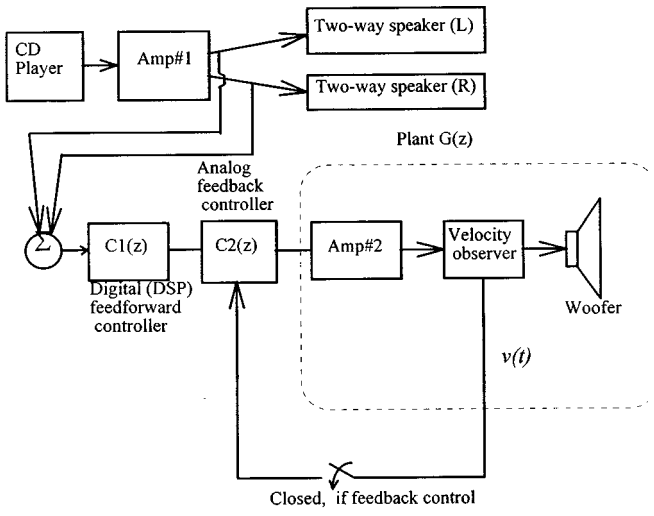

FIG. 6. Total system diagram of the bass-enhanced audio system.

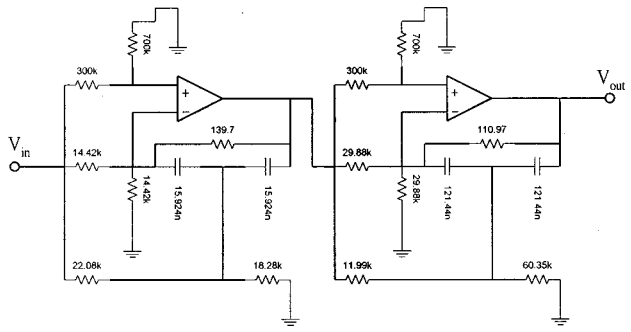

FIG. 8. Circuit diagram of the H_∞ feedback controller.

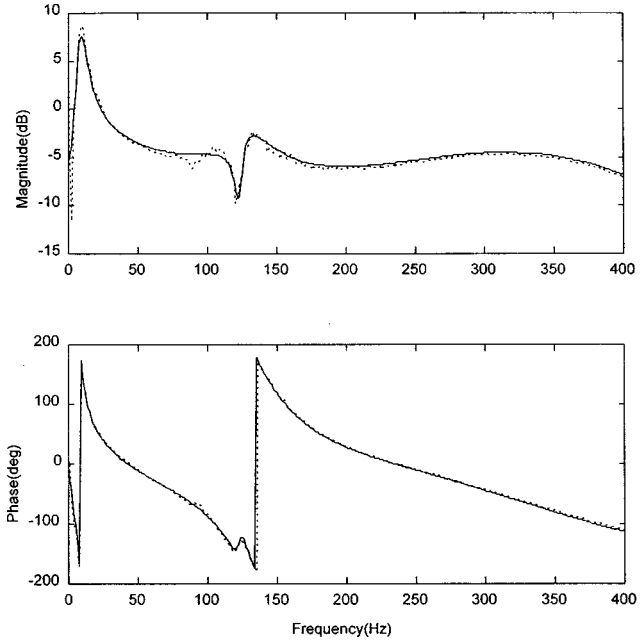

FIG. 9. Comparison between the measured and the regenerated frequency responses of the feedback-compensated plant. Measured data ———; regenerated data —.

by giving more weight to the low-frequency response of the feedforward controller. After a subjective evaluation, we felt a boosted bass would give a more impressive sense of ''super bass'' than just a flat response. To test the practicality of the proposed system, a pop music sample is used as the command signal to evaluate the tracking performance of the hybrid controller. The time-domain responses for the uncompensated system and the compensated system are compared in Fig. 13. It is evident from the comparison that the proposed system indeed produces more satisfactory tracking performance.

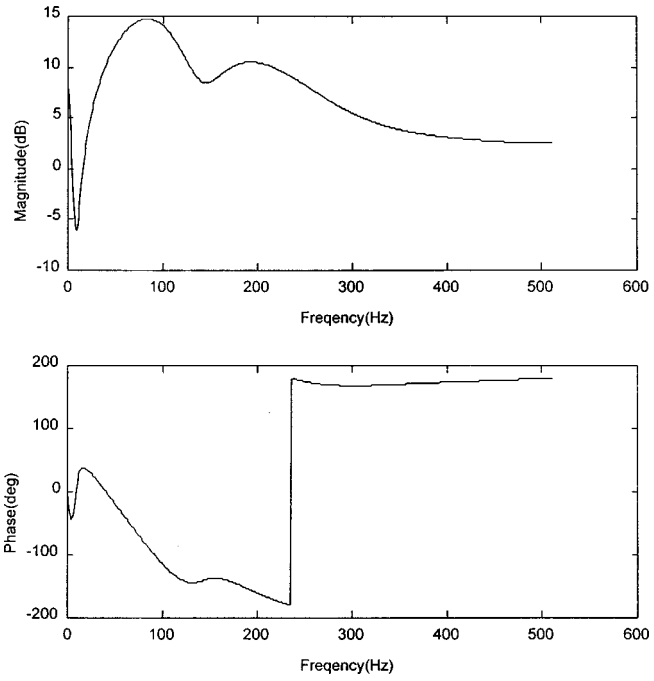

FIG. 10. Frequency response of the H_2 feedforward controller.

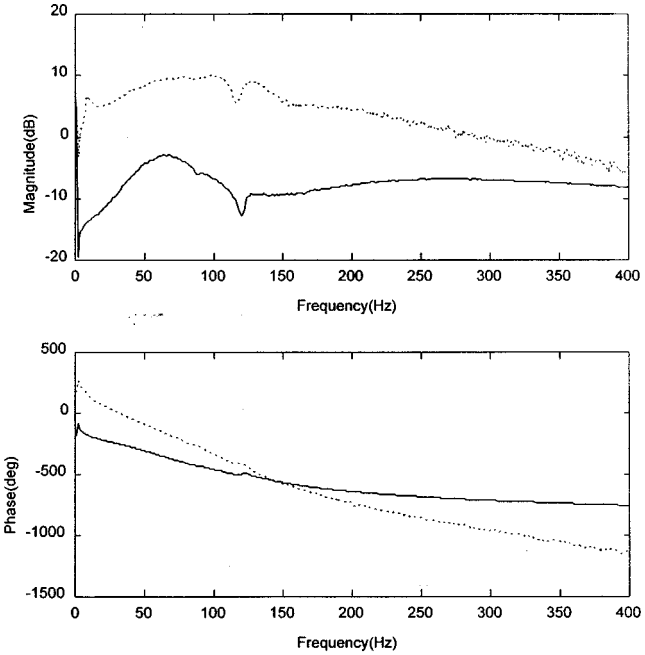

FIG. 11. Frequency responses between a white noise input and the cone velocity output for the uncompensated system and the compensated system. Control off —; control on ———.

IV. CONCLUSIONS

Modern control techniques are exploited to enhance the low-frequency performance of moving-coil loudspeakers, under the electromagnetic properties and acoustical constraints. A self-sensing velocity observer is developed for cone velocity estimation without additional motional or acoustical sensors. H_∞ feedback control is employed for robust stabilization, while the H_2 feedforward model matches

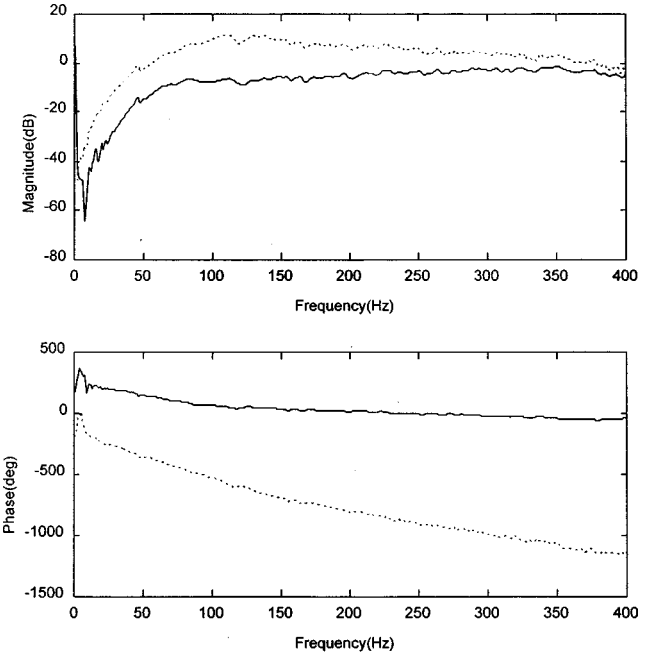

FIG. 12. Frequency responses between a white noise input and the far-field sound pressure output for the uncompensated system and the compensated system. Control off —; control on ———.

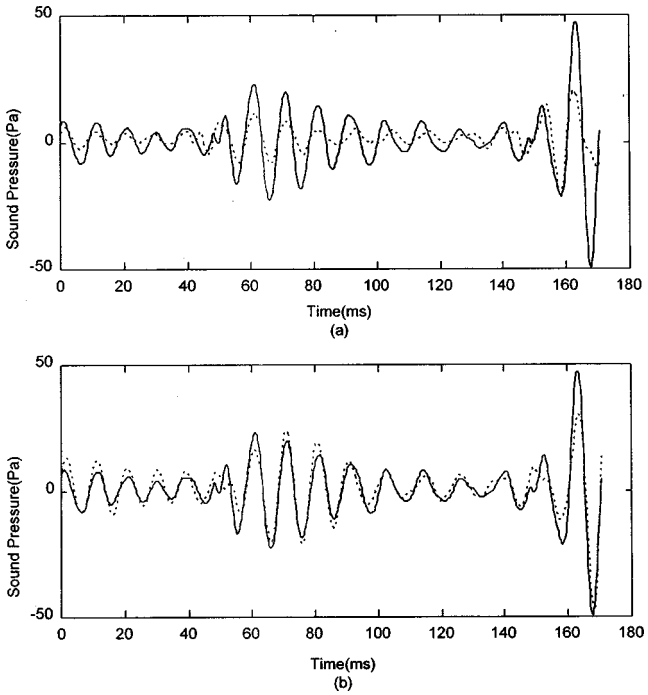

FIG. 13. Time-domain tracking performance of the bass-enhanced system for the pop music signal. (a) Command signal versus sound pressure output signal before bass compensation; (b) Command signal versus sound pressure output signal after bass compensation. Command signal — output signal ———.

control for tracking performance. The results obtained in experiments indicate that the proposed system yields improved performance over the uncompensated one. However, as a limitation of the proposed methodology, the success of this method relies on adequate design of the original mechanical system and acoustical system (such as a sufficiently large diameter of the speaker). That is, one can never adequately control a poorly designed mechanical system. Overemphasis on the proposed electronic compensation will likely result in undesirable nonlinearity in the system.

Although this paper mainly focuses on audio loudspeakers, the same rationale can be extended to the other applications, e.g., control speakers for active noise cancellation, linear electromagnetic actuators for active vibration control and isolation, where efficient low-frequency response is crucial. Since the research was originally targeted at the subwoofer, only one driver was tested. However, the feasibility of the proposed technique applied to the systems of multiple drivers should be examined. Future research is planned in these areas.

ACKNOWLEDGMENTS

We wish to thank Dr. William Thompson, Jr. of Applied Research Laboratory, Penn State University for providing class notes on acoustic transducers. The work was supported by the National Science Council in Taiwan, Republic of China, under the Project No. NSC 86-2212-E-009-003.

Aström, J., and Wittenmark, B. (**1990**). *Computer-Controlled Systems* (Prentice-Hall, Englewood Cliffs, NJ).

Bai, M. R., and Lin, H. H. (**1997**). ''Comparison of active noise control structures in the presence of acoustical feedback by using the H_∞ synthesis technique,'' J. Sound Vib. **206**, 453–471.

Beranek, L. L. (**1954**). *Acoustics* (McGraw-Hill, New York).

Borwick, J. (**1994**). *Loudspeaker and Headphone Handbook* (Butterworth-Heinemann, Oxford).

Colloms, M. (**1991**). *High Performance Loudspeakers* (Wiley, New York).

Doyle, J. C., Francis, B. A., and Tannenbaum, A. R. (**1992**). *Feedback Control Theory* (Macmillan, New York).

Juang, J. N. (**1994**). *Applied System Identification* (Prentice-Hall, Englewood Cliffs, NJ).

Kinsler, L. E., Frey, A. R., Coppens, A. B., and Sanders, J. V. (**1982**). *Fundamentals of Acoustics* (Wiley, New York).

Kuriyama, J., and Furukawa, Y. (**1989**). ''Adaptive loudspeaker system,'' J. Audio Eng. Soc. **37**, 919–926.

Okada, Y., Matsuda, K., and Hashitani, H. (**1995**). ''Self-sensing active vibration control using the moving-coil-type actuator,'' ASME J. Vib. Acoust. **117**, 411–415.

Morari, M., and Zafirou, E. (**1989**). *Robust Process Control* (Prentice-Hall, Englewood Cliffs, NJ).

Radcliffe, J., and Gogate, S. D. (**1992**). ''Identification and modeling of speaker dynamics for acoustic control application,'' ASME J. Vib. Acoust. **38**, 295–300.

Schaumann, R., Ghausi, M. S., and Laker, K. R. (**1989**). *Design of Analog Filters: Passive, Active RC, and Switched Capacitor* (Prentice-Hall, Englewood Cliffs, NJ).

Small, R. H. (**1972**). ''Closed-box Loudspeaker Systems, Part I: Analysis,'' J. Audio Eng. Soc. **20**, 798–808.